

# Spectroelectrochemical Raman Study of a Novel Well-Barrier-Well Vinylene-Bridged-Octithiophene Oligomer: An Analysis of the Conjugation Length and of the Electronic Defects Created upon Doping

J. Casado,<sup>†</sup> J. J. Maraver Puig,<sup>†</sup> V. Hernández,<sup>‡</sup> G. Zotti,<sup>§</sup> and J. T. López Navarrete<sup>\*‡</sup>

Departamento de Ingeniería Química, Química Física y Química Orgánica, Escuela Politécnica Superior, Universidad de Huelva, 21819-La Rábida, Huelva, Spain, Departamento de Química Física, Universidad de Málaga, 29071-Málaga, Spain, and Istituto di Polarografia ed Elettrochimica Preparativa, Consiglio Nazionale delle Ricerche, c.o. Stati Uniti 4, 35020-Padova, Italy

Received: June 7, 2000; In Final Form: August 23, 2000

We have studied the Fourier transform Raman (FT-Raman) spectra of a novel well-barrier-well vinylene-bridged-octithiophene in neutral and doped states. The compound was doped in a reaction with iodine vapors and electrochemically in the form of a thin film coated platinum electrode. We have analyzed the evolution of the Raman spectral pattern upon oxidation of the material at different anodic potentials. The data indicate that the oxidation process takes place in two well-differentiate steps: the initial formation of the radical cation followed by the generation of the dication. The comparison of the spectroscopic data with those previously obtained on a related vinylene-bridged-quaterthiophene enabled us to draw conclusions about the effective  $\pi$ -conjugation length in neutral state. RHF/3-21G\* theoretical calculations have been performed to analyze the changes of the geometrical parameters when going from the neutral to the doped forms.

## I. Introduction

Polyconjugated organic molecules constitute a promising class of materials for advanced technological applications such as nonlinear-optical devices,<sup>1</sup> field-effect transistors,<sup>2–4</sup> and light-emitting diodes.<sup>5–8</sup> These new materials are characterized by a low difference in energy between the HOMO and the LUMO molecular orbitals (energy gap), which determines the degree of conjugation and mobility of the  $\pi$ -electrons along the molecular backbone (molecular polarizability), linear and nonlinear optical properties, etc. Polymeric materials have been the leader molecules in this field even when they present too much inconvenients such as broad chain length distributions, low crystallinity and solubility, chemical defects, etc. To avoid these problems, many classes of  $\pi$ -conjugated oligomers have been studied over the past decade. Analyzing these materials, it is possible to establish a precise relationship between the physical or chemical properties and the chemical architecture (i.e., relationship between energy gap and conjugation): this strategy is known as the *oligomeric approach*.<sup>9</sup> The alternation in the conjugated backbone of an oligomer of different electronic segments with various energy gaps gives molecules with excellent optical and electrical properties.<sup>10</sup> If A and B are two conjugated segments, with different energy gaps, the search for polyconjugated cooligomers  $A_nB_m$  with regular sequences of A and B is at present a promising way to develop new materials with potentials applications as materials for quantum wells in photonics.<sup>5</sup> A variety of conjugated cooligomers derived from the combination of benzene and pyrrol, benzene and thiophene, ethylene and thiophene or pyrrol, etc., have already been studied.

The energy gaps of cooligomers of the type  $A_nB_m$  cannot be estimated from the analysis of the electronic spectra or redox potentials only, but other magnitudes must be studied or

analyzed. Raman spectra of polyconjugated organic materials show for some few lines selective intensity enhancement and frequency and intensity dispersions with conjugation length. For low energy gap conjugated oligomers having a nondegenerated electronic ground-state, *effective conjugation coordinate* theory (ECC) predicts that there exists a unique vibrational coordinate which strongly couples with the  $\pi$ -conjugation.<sup>12–15</sup> Thus, Raman spectroscopy becomes a powerful technique to analyze the extent of the conjugation in neutral state and the nature of the charged defects created in doped conjugated molecules or in low energy gap segmented electronic molecules.

During years, spectroscopists have made use of quantum mechanical methods to interpret their experimental data. The current methods are able to give reliable information about the molecular structure and properties not only for neutral systems but also for ionized molecules. Most calculations are carried out into the *ab initio* Hartree–Fock (HF) scheme. For large molecular systems, at this level of theory, the predicted quantities usually differ from the experimental ones due to a combination of electron correlation effects and basis set deficiencies. However, this scheme is still useful to get orientative trends about the changes induced by the ionization of the system with respect to the neutral pattern molecule (e.g., to simulate different oxidation states).<sup>16</sup>

In the past, a noticeable amount of research has been performed on  $\pi$ -conjugated organic copolymers and cooligomers.<sup>20–23</sup> We have recently reported on the vibrational spectra of a cooligomer consisting of two bithienyl (T2) parts connected through a vinylene bridge (V) in relation to the effective conjugation length of the compound in neutral and doped states.<sup>20,21</sup> This well-barrier-well T2VT2 molecule can be interpreted like two end moieties with a lower energy gap than the central vinylene spacer.

In this article, we study, by means of FT-Raman spectroscopy, a new well-barrier-well vinylene-bridged-octithiophene, (T2VT2)<sub>2</sub>, both in the neutral and doped states, which can be considered

\* To whom correspondence should be addressed.

<sup>†</sup> Departamento de Ingeniería Química.

<sup>‡</sup> Departamento de Química Física (fax: ++ 34-952-132000).

<sup>§</sup> Istituto di Polarografia ed Elettrochimica Preparativa.

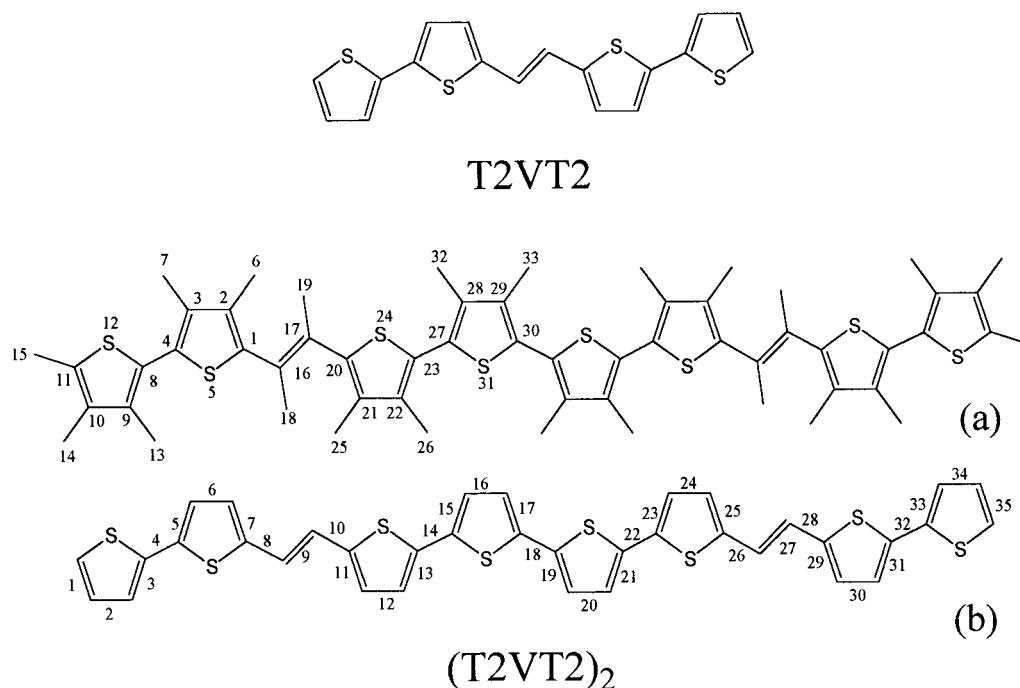


**Figure 1.** Chemical structure of (T2VT2)<sub>2</sub> and its monomer T2VT2. (a) Atom numbering corresponds to that appearing in Table 3. (b) Bond numbering corresponds to that appearing in Figures 5 and 6.

as the dimer of the T2VT2 cooligomer previously studied. As a support to the experimental data, we also present the results of a comparative quantum-mechanical study performed on the neutral form of the compound and on its radical cation and dication species to analyze the effects of the ionization on the molecular structure.

## II. Experimental and Computational Details

The chemical structure of (T2VT2)<sub>2</sub>, is depicted in Figure 1. The synthesis and purification methods are described elsewhere.<sup>22</sup> Chemical oxidation was carried out, under dry atmosphere, by slow in situ sublimation of iodine at room temperature, using a solid–vapor doping technique.<sup>23</sup> Electrochemical doping was carried out on samples as solid films deposited on the working electrode from a 1,2-dichloromethane dispersion, followed by slow solvent evaporation.

Electrochemical experiments were performed in analytical grade acetonitrile (from Aldrich). Tetrabutylammonium tetrafluoroborate (TBAT) was used as the supporting electrolyte in 0.1 M concentration. A platinum sheet (1 cm<sup>2</sup> area) was the working electrode, a second platinum sheet was the counter electrode and a saturated calomel electrode (SCE) was the reference electrode. The experimental procedure was as follows: the coated platinum electrode was immersed into the 0.1 M TBAT acetonitrile solution, and a fixed anodic potential was applied during 60 s. The voltammetric wave of (T2VT2)<sub>2</sub> (Figure 2) previously reported by Berlin and Zotti<sup>22</sup> was used to choose the anodic potentials values for the selective oxidation of the film. A Voltalab40 electrochemical equipment from Radiometer was employed.

FT-Raman spectra were measured at room temperature using the FT-Raman accessory kit (FRA/106-S) of a Bruker Equinox 55 FT-IR interferometer. A continuous-wave Nd:YAG laser working at 1064 nm was employed for Raman excitation. A germanium detector operating at liquid nitrogen temperature was used. Raman scattering radiation was collected in a backscattering configuration with a standard spectral resolution of 4 cm<sup>-1</sup>. To avoid possibly damaging the sample upon laser radiation, the laser beam was loosely focused on the sample

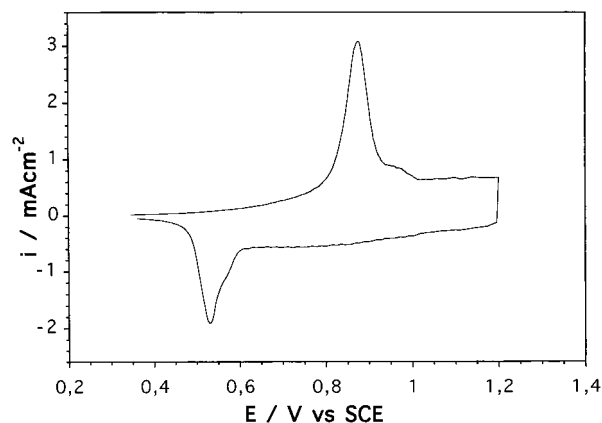


**Figure 2.** Voltammetric wave of (T2VT2)<sub>2</sub>. From ref 22.

and its power was kept at a level lower than 30 mW. In all Raman experiments, 1000 scans were added to improve the signal-to-noise ratio. Raman spectra of the neutral and chemically oxidized materials were obtained for powdered samples in sealed capillaries, and for the iodine doped (T2VT2)<sub>2</sub>, just after carrying out the exhaustive oxidation with iodine vapors. On the other hand, the Raman spectra of the electrochemically doped samples were recorded directly on the platinum electrode.

Calculations were carried out at the HF level using the 3-21G\*<sup>24</sup> basis set as implemented in the GAUSSIAN 98<sup>25</sup> suite of programs with a SGI Origin 2000 supercomputer. Geometry optimizations were performed on isolated entities; the neutral and doubly ionized forms were treated as closed shell systems (RHF), while the singly ionized species was treated as an open shell system (ROHF). All computed molecular structures were optimized under the constraints of keeping: (a) the planarity of the whole molecule and (b) the all-anti conformation of the thiophene units.

## III. (T2VT2)<sub>2</sub> in Neutral State.

The Raman spectra of the neutral forms of (T2VT2)<sub>2</sub> and T2VT2 are shown in Figure 3. Both spectra show the charac-

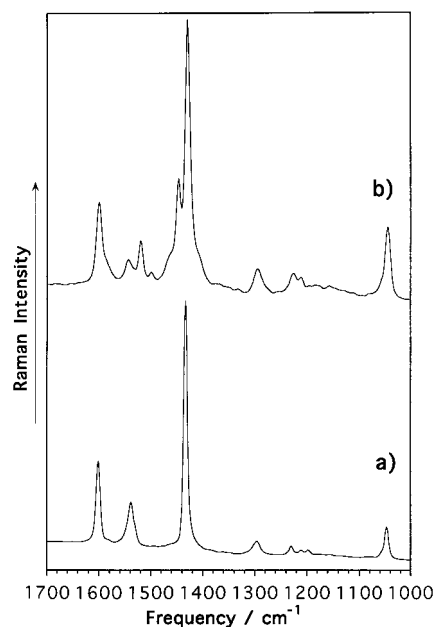


**Figure 3.** Raman spectra of (a) T2VT2 and (b) (T2VT2)<sub>2</sub> in neutral state in 1700–1000 cm<sup>-1</sup> spectral range.

**TABLE 1: Correlation between the Vibrational Raman Frequencies (in cm<sup>-1</sup>) of Neutral (T2VT2)<sub>2</sub>, T2VT2,  $\alpha,\alpha'$ -Dimethylquaterthiophene, and  $\alpha,\alpha'$ -Dimethylquinquethiophene**

(T2VT2) <sub>2</sub>	(T2VT2) <sup>a</sup>	DMQiT <sup>b</sup>	DMQqT <sup>b</sup>	assignment <sup>c</sup>
1599	1601			$\nu(\text{C}=\text{C})_{\text{trans-vinylene}}$
1544				
1519	1539	1533	1525	line A
1499				
1446		1448	1450	line C
1429	1433	1482	1481	line B
1295	1296			$\delta_s(\text{C}-\text{H})_{\text{trans-vinylene}}$
1225	1230	1224	1219	$\nu(\text{C}-\text{C})_{\text{inter-ring}}$
1210	1210			
1045	1047	1044	1044	line D

<sup>a</sup> Data from ref 20. <sup>b</sup> Data from ref 28. <sup>c</sup>  $\nu$  = stretching;  $\delta$  = in-plane bending; s = symmetric.

teristic features common to many other classes of conjugated oligomers,<sup>27,28</sup> that is, only a few Raman lines are experimentally observed despite the complex chemical structures. Another peculiarity of the conjugated systems is that, of the usually large population of Raman-active modes predicted by the optical selection rules, the very few ones experimentally observed are overwhelmingly strong in the aromatic C=C stretching region. Table 1 summarizes the frequencies measured in the Raman spectra of (T2VT2)<sub>2</sub> and T2VT2, together with those of a series of  $\alpha,\alpha'$ -dimethyloligothiophenes of variable lengths previously studied like prototypes of nonintercalated oligomers.<sup>20,27,28</sup>

The line at 1599 cm<sup>-1</sup> of (T2VT2)<sub>2</sub> can be assigned to a symmetric stretching of C=C of the vinylene groups. The corresponding vibration in T2VT2 appears at 1601 cm<sup>-1</sup> and is absent in the spectra of the nonintercalated oligothiophenes. This  $\nu(\text{C}=\text{C})_{\text{vinylene}}$  vibration slightly downshifts from T2VT2 to (T2VT2)<sub>2</sub> (by 2 cm<sup>-1</sup>); however, it undergoes a sizable dispersion to lower frequencies with respect to the bis(thienyl)-vinylene compound (TVT),<sup>26</sup> where it appears at 1618 cm<sup>-1</sup>. These data suggest that the conjugated thienyl moieties longer than a dimer do not affect considerably the electronic structure of the vinylene spacer, the main modifications taking place on going from the monomeric to the dimeric thienyl-moieties. On the other hand, the band at 1295 cm<sup>-1</sup> may be assigned to a

symmetric bending mode of the C–H bonds attached to the vinylenic spacers.

Around 1520 cm<sup>-1</sup> appears the usually termed as *line A*.<sup>23,28</sup> In the case of T2VT2 the corresponding Raman-active vibration was observed at 1539 cm<sup>-1</sup> and assigned, on the basis of the RHF/6-31G\*\* theoretical eigenvectors, as a totally symmetric  $\nu_{\text{as}}(\text{C}=\text{C})$  mode mainly localized on the two outer rings. For (T2VT2)<sub>2</sub>, line A disperses 20 cm<sup>-1</sup> downward with respect to T2VT2. A similar downshift was observed in the  $\alpha,\alpha'$ -dimethyloligothiophenes, where the related line A dispersed by 21 cm<sup>-1</sup> to lower frequencies on going from the trimer to the pentamer.<sup>23,28</sup> After dimerization, one of the two bithienyl moieties of T2VT2 becomes a tetramer and the vibration assigned to line A further downshifts as a consequence of the increased  $\pi$ -conjugation

The so-called *line B* is always the strongest one of the spectrum.<sup>20,23,28</sup> In the  $\alpha,\alpha'$ -dimethyloligothiophenes it appears at around 1480 cm<sup>-1</sup>, while it is measured at 1429 cm<sup>-1</sup> in (T2VT2)<sub>2</sub> and at 1433 cm<sup>-1</sup> in T2VT2. The vibration assigned to this band was described, as derived from the theoretical eigenvectors,<sup>20,23</sup> as a fully in-phase symmetric  $\nu_s(\text{C}=\text{C})$  mode spreading over the whole conjugated chain. In the effective conjugation coordinate theory,<sup>13–15</sup> the Raman ECC mode selectively enhanced is defined like an in-phase oscillation of the alternating C=C/C–C bonds of the  $\pi$ -conjugated molecular backbone. In agreement with this definition, the vibration associated with line B can be assigned as the ECC mode.

The band at 1446 cm<sup>-1</sup> of (T2VT2)<sub>2</sub> does not have counterpart in the Raman spectrum of T2VT2. The members of the series of the  $\alpha,\alpha'$ -dimethyl end-capped oligothiophenes show a Raman scattering at around 1445 cm<sup>-1</sup>, which shows a slight upshift and intensity enhancement with increasing chain length, that is absent in the series of nonintercalated  $\alpha$ -linked oligothiophenes.<sup>11</sup> This band, usually termed as *line C*, has been observed in many classes of  $\alpha$  or  $\beta$  end-capped oligothiophenes<sup>27,28</sup> and assigned to a  $\nu_s(\text{C}=\text{C})$  vibration, mostly localized on the inner rings, for which the motions of the successive thiophene units are completely out-of-phase.<sup>23</sup> In the case of (T2VT2)<sub>2</sub> we think that the scattering at 1446 cm<sup>-1</sup> has to be assigned to a vibration of the central quaterthiophene moiety of the same type as that described above.

Finally, *line D* appears for all oligothiophenes as a sharp band (or doublet) of medium intensity at around 1050–1080 cm<sup>-1</sup>. This vibration has been assigned as a totally symmetric in-phase bending mode of the C–H bonds attached at the different  $\beta$ -positions of the  $\pi$ -conjugated backbone.<sup>20,23,28</sup> For the (T2VT2)<sub>2</sub> cooligomer, this characteristic vibration is measured at 1045 cm<sup>-1</sup>.

The voltammetric data recorded by Berlin and Zotti<sup>22</sup> show that on going from T2VT2 to (T2VT2)<sub>2</sub>, the oxidation potentials decreases by around 0.2–0.3 V. The same authors report that the maximum absorption band in the UV–vis spectrum of (T2VT2)<sub>2</sub> undergoes a bathochromic shift by around 80–100 nm with respect to T2VT2.<sup>22</sup> These results are in full agreement with the Raman data of the neutral (T2VT2)<sub>2</sub>, and indicate that after dimerization the effective conjugation length increase, thus making this well-barrier-well bridged vinylene-octithiophene a good candidate for optical and electrical applications.

#### IV. Doped (T2VT2)<sub>2</sub>.

Figure 4 shows the comparison between the Raman spectrum of the neutral form of (T2VT2)<sub>2</sub> and those obtained on different samples electrochemically oxidized at increasing anodic potentials and just after the exhaustive oxidation with dry iodine vapors. Table 2 summarizes a correlation between the frequen-



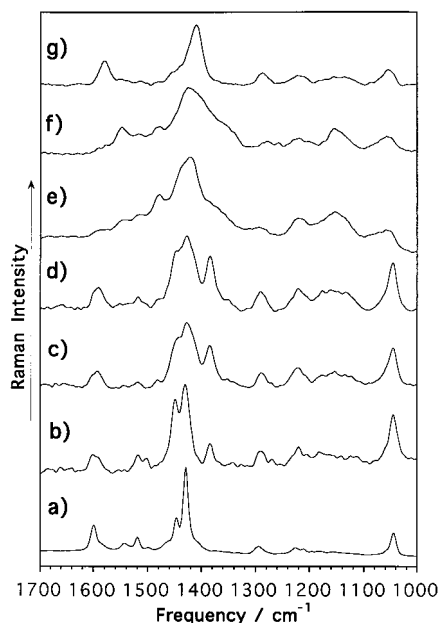


**Figure 4.** Raman spectra of (a) the neutral (T2VT2)<sub>2</sub> together with the electrochemical doped (T2VT2)<sub>2</sub> at various anodic potentials levels (in V, versus SCE): (b) 0.3 V, (c) 0.5 V, (d) 0.7 V, (e) 1.0 V, (f) 1.2 V; (g) Raman spectrum of iodine-oxidized (T2VT2)<sub>2</sub>.

cies measured in the whole series of spectra together with those previously determined in the Raman spectra of the radical cations of T2VT2<sup>21</sup> and of the  $\alpha,\alpha'$ -dimethylquinquethiophene (DMQqT).<sup>29,30</sup>

The band measured at 1581 cm<sup>-1</sup> in iodine-doped (T2VT2)<sub>2</sub> can be correlated to that observed at 1585 cm<sup>-1</sup> in T2VT2 radical cation, being due to a pure  $\nu(\text{C}=\text{C})$  vibration of the transvinylene bridges.<sup>21</sup> The frequency of this mode progressively decreases with increasing oxidation potential: from around 1600 cm<sup>-1</sup> at 0.3 V to 1590 cm<sup>-1</sup> at 1.0 V. The sizable downshift of this vibration by about 20 cm<sup>-1</sup> on going from the neutral form to the iodine-doped species is a consequence of the gradual loss of double bond character of the vinylenic spacers induced by the quinoidization of the  $\pi$ -conjugated backbone upon doping.

The most intense scattering in the Raman spectrum of the iodine-doped (T2VT2)<sub>2</sub> is a broad band centered at 1410 cm<sup>-1</sup>, while for the sample electrochemically oxidized at 1.2 V it is recorded at 1422 cm<sup>-1</sup>. This band must be correlated with the Raman line at 1429 cm<sup>-1</sup> in the neutral form of (T2VT2)<sub>2</sub> and with that at 1411 cm<sup>-1</sup> in iodine-doped T2VT2, and assigned as line B of the oxidized sample. The vibration likely extends over the whole molecule, and seems to be sensitive to the nature of the counterion. The band appears at higher frequency values (1428–1422 cm<sup>-1</sup>) when the counterion is a bulky group like tetrafluoroborate and at lower frequency (around 1410 cm<sup>-1</sup>) when the counterion is an iodine-reduced species (I<sup>-</sup>, I<sub>3</sub><sup>-</sup> or I<sub>5</sub><sup>-</sup>) which allows for a more close approximation of the counterion to the doped  $\pi$ -conjugated spine of the molecule (probably in the proximity of the vinylene spacers, where the steric hindrance is lower), and thus for a more pronounced electrostatic interaction.

The band measured at 1385 cm<sup>-1</sup> in the of (T2VT2)<sub>2</sub> oxidized to 0.3, 0.5, and 0.7 V may be ascribed to an intra-ring  $\nu(\text{C}-\text{C})$  vibration which gains a partial double bond character upon quinoidization of the  $\pi$ -conjugated skeleton. The band at 1290 cm<sup>-1</sup> can be assigned to the symmetric in-phase  $\delta_s(\text{CH})$  in-plane bending of the vinylene bridges, whereas those measured around 1220, 1180, and 1160 cm<sup>-1</sup> could be assigned to interring  $\nu(\text{C}-\text{C})$  modes with different phases which gain intensity

upon oxidation. Finally, the Raman scattering observed at 1050 cm<sup>-1</sup> is due to the totally symmetric  $\delta_s(\text{CH})$  of the thiophene rings, being clearly correlated with the typical line D of the neutral sample. This band also shows a dispersion to higher frequencies with increasing oxidation degree: from 1046 cm<sup>-1</sup> (0.3 V–0.5 V) and 1058 cm<sup>-1</sup> (1.0 V–1.2 V) to 1056 cm<sup>-1</sup> for the iodine-doped sample.

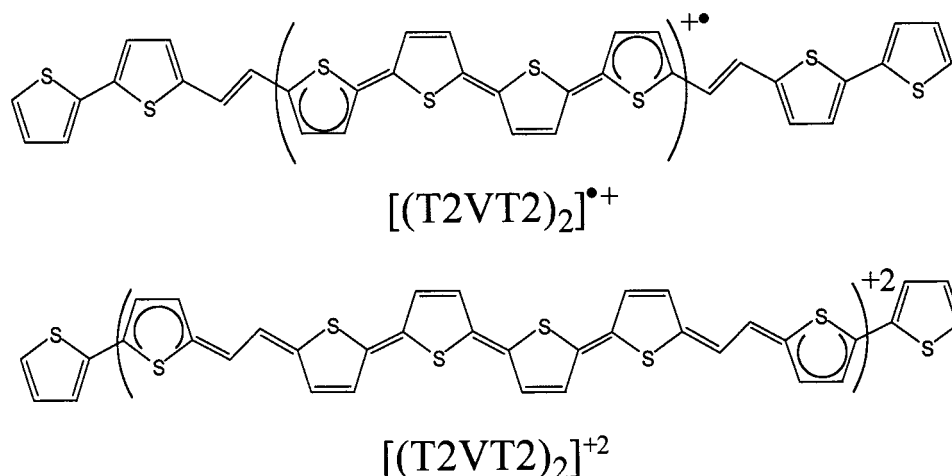
The previously published cyclic voltammetric study of (T2VT2)<sub>2</sub> displayed a reversible electrochemical wave which shows the oxidative maximum around 0.8 V and the reductive maximum around 0.6 (versus SCE).<sup>22</sup> As a consequence, the chemical doping of (T2VT2)<sub>2</sub> with iodine vapors could progress to the highest oxidation state since the oxidation potential for the system I<sub>2</sub>/I<sup>-</sup> is larger than the oxidation peak of (T2VT2)<sub>2</sub> (i.e.,  $\epsilon^\circ(\text{I}_2/\text{I}^-) = 0.812$  V versus SCE).<sup>31</sup>

The resemblance between the Raman spectra of (T2VT2)<sub>2</sub> oxidized at 0.5 and 0.7 V, by one hand, and between the Raman spectra of the iodine-doped T2VT2, iodine-doped (T2VT2)<sub>2</sub> and (T2VT2)<sub>2</sub> oxidized at 1.0 and 1.2 V, on the other hand, suggests the generation of two different types of charged defects. It is likely that at low anodic potentials a radical cation is created in the central quaterthienyl moiety which slightly affects the structure of the vinylene spacers or of the bithienyl end-moieties (see Chart 1). A dicationic charged defect could instead be created at high anodic potentials or upon doping with iodine. In the latter case the structure of the whole  $\pi$ -conjugated system should undergo sizable modifications with respect to the neutral molecule in order to mitigate the repulsive interactions between the two positive charges (see Chart 1).

This spectroelectrochemical Raman study reveals that (T2VT2)<sub>2</sub> undergoes a two-electron oxidation, consisting in the initial oxidation of the cooligomer to the radical cation followed by the subsequent oxidation to the dication. Our spectroscopic data agree with the electrochemical and UV–vis–NIR results reported by Roncali et al. on a related series of oligothiophenevinylene which provided the first evidence for a two-electron generation of a dication in  $\pi$ -conjugated oligomers based on the repetition of a single basic unit.<sup>18,19</sup> These authors suggested that this type of compounds could be of interest for modeling bipolarons in conjugated polymers. This work highlights the possibility of using oligothiophene blocks separated from each other by a vinylene spacer to model different types of charged-defects (i.e., polarons or bipolarons) in conducting polymers.

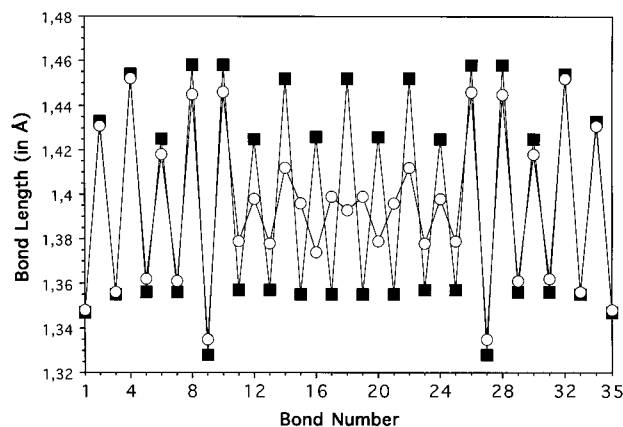
## V. Molecular Geometry Optimizations

The RHF/3-21G\* optimized molecular structure of neutral (T2VT2)<sub>2</sub> shows that all the inner thiophene rings display almost the same geometry, which slightly differs from that found in the bithienyls outer parts (see Figures 5 and 6). The main geometrical changes upon ionization concern the distortions of the  $\pi$ -conjugated CC bonds. The ROHF/3-21G\* optimized geometry of the radical cation indicates the formation of a positive polaron type defect localized in the middle of the molecule and extending over the quaterthienyl central part (see Figure 5). This charged species is characterized by the partial reversal of the single-double CC bond alternation pattern of the central thiophene rings of the molecule. The amplitude of the structural modifications progressively decrease away from the center of the cooligomer. On the other hand, the RHF/3-21G\* optimized geometry of the dication shows the formation of a positive bipolaron type defect which extends not only over the quaterthienyl central part but also over the vinylene spacers and the bithienyl end-moieties (see Figure 6). The amplitude of the structural modifications in the dicationic species little affects

**CHART 1: Approximate Chemical Structures of the Molecular Domain Perturbed by the Ionization in the Radical Cation and Dication of (T2VT2)<sub>2</sub> as Deduced from the Theoretical Geometry Optimizations****TABLE 2: Correlation between the Vibrational Raman Frequencies (in cm<sup>-1</sup>) of Electrochemical Oxidized (T2VT2)<sub>2</sub> at Various Anodic Potentials Levels (in V, versus SCE), Iodine-Oxidized (T2VT2)<sub>2</sub>, Iodine-Oxidized T2VT2, and Iodine-Oxidized α,α'-Dimethylquaterthiophene and α,α'-Dimethylquinquethiophene**

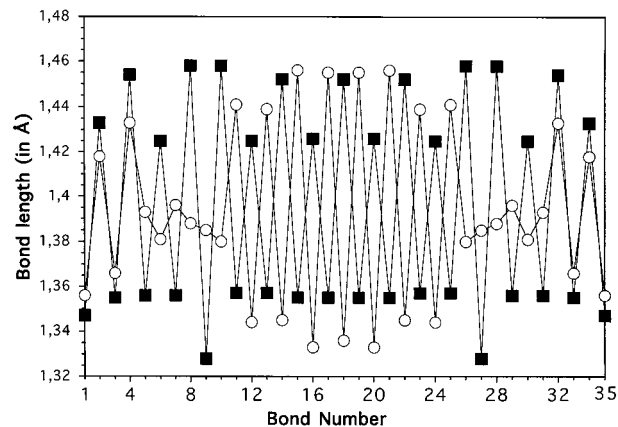
0.3	0.5	0.7	1.0	1.2	(T2VT2) <sub>2</sub> -I <sub>2</sub>	T2VT2-I <sub>2</sub> <sup>a</sup>	DMQqT-I <sub>2</sub> <sup>b</sup>	DMQqT-I <sub>2</sub> <sup>b</sup>	assignment <sup>c</sup>
1602	1593	1592	1590		1581	1585			$\nu_s(\text{C}=\text{C})$
1449	1446	1446	1435			1448	1438		
1429	1431	1428	1423	1422	1410	1411	1417	1420	line B
1385	1385	1385							
1292	1291	1291	1286	1292	1287	1287			
1221	1221	1221	1221	1219	1223	1223	1220	1226	
	1177	1176							
	1163	1153	1157	1156		1161	1164		
1045	1046	1046	1058	1058	1056		1050	1050	line D

<sup>a</sup> Data from ref 21. <sup>b</sup> Data from ref 23. <sup>c</sup>  $\nu$  = stretching; s = symmetric.

**Figure 5.** HF/3-21G\* optimized CC bond lengths of the (T2VT2)<sub>2</sub> in the neutral form (filled squares) and in the radical cationic form (open circles). For bond numbering, see Figure 1b. ROHF method has been used for the open-shell systems.

however the outermost thiophene rings of the molecule. The sizable geometrical changes on going from the neutral form to the dication, together with the expected changes in the force constants associated with the different CC bonds of the  $\pi$ -conjugated backbone, could account for the noticeable dispersions to lower frequencies upon oxidation of the few totally symmetric Raman-active modes experimentally observed.

Table 3 compares the Mulliken atomic charges of the neutral (T2VT2)<sub>2</sub> and its radical cation and dication. The positive charges on the sulfur atoms experience the largest changes upon ionization. This is a consequence of the ease with which the sulfur atom varies its electron density. In particular, the charges

**Figure 6.** HF/3-21G\* optimized CC bond lengths of the (T2VT2)<sub>2</sub> in the neutral form (filled squares) and in the dicationic form (open circles). For bond numbering, see Figure 1b.

of the inner S<sub>24</sub> and S<sub>31</sub> atoms increase by 0.060 and 0.067 *e* from the neutral form to the radical cation, while the charges of the S<sub>5</sub>, S<sub>12</sub>, and S<sub>24</sub> atoms in the dication are larger than those of the neutral molecule by 0.091, 0.070, and 0.071 *e*, respectively. The theoretical data indicate that the S atoms in (T2VT2)<sub>2</sub> act as electron donors. The C atoms of the  $\pi$ -conjugated backbone are negatively charged in the three systems. Larger negative charges are found for the C atoms placed at  $\alpha$ -positions of the rings, and those placed at the end  $\alpha$ -positions of the molecule display by far the largest values in all the cases. The charges on the C<sub>16</sub>, C<sub>20</sub>, and C<sub>27</sub> atoms increase by ca. 0.043 *e* and those on the hydrogens attached at the  $\beta$ -positions of the

**TABLE 3: Mulliken Atomic Charges Calculated at the HF/3-21G\* Level for the Neutral, Radical Cationic, and Dicationic Forms of (T2VT2)<sub>2</sub><sup>a</sup>**

atom	neutral	radical cation	dication
C <sub>11</sub>	-0.482	-0.475	-0.454
C <sub>10</sub>	-0.233	-0.234	-0.240
C <sub>9</sub>	-0.244	-0.234	-0.199
C <sub>8</sub>	-0.285	-0.296	-0.331
S <sub>12</sub>	0.467	0.485	0.537
H <sub>15</sub>	0.271	0.283	0.310
H <sub>14</sub>	0.254	0.265	0.289
H <sub>13</sub>	0.258	0.261	0.282
C <sub>4</sub>	-0.298	-0.283	-0.240
C <sub>3</sub>	-0.231	-0.238	-0.251
C <sub>2</sub>	-0.228	-0.201	-0.143
C <sub>1</sub>	-0.312	-0.340	-0.380
S <sub>5</sub>	0.508	0.535	0.603
H <sub>7</sub>	0.262	0.275	0.304
H <sub>6</sub>	0.250	0.260	0.296
C <sub>16</sub>	-0.198	-0.155	-0.107
C <sub>17</sub>	-0.201	-0.238	-0.287
H <sub>18</sub>	0.246	0.262	0.290
H <sub>19</sub>	0.246	0.259	0.276
C <sub>20</sub>	-0.310	-0.269	-0.222
C <sub>21</sub>	-0.229	-0.245	-0.242
C <sub>22</sub>	-0.230	-0.178	-0.149
C <sub>23</sub>	-0.299	-0.346	-0.346
S <sub>24</sub>	0.510	0.570	0.581
H <sub>25</sub>	0.251	0.275	0.291
H <sub>26</sub>	0.261	0.286	0.310
C <sub>27</sub>	-0.294	-0.251	-0.252
C <sub>28</sub>	-0.232	-0.234	-0.252
C <sub>29</sub>	-0.231	-0.184	-0.179
C <sub>30</sub>	-0.295	-0.305	-0.297
S <sub>31</sub>	0.522	0.589	0.546
H <sub>32</sub>	0.232	0.299	0.307
H <sub>33</sub>	0.262	0.300	0.305

<sup>a</sup> For atom numbering, see Figure 1a. The ROHF method has been used for the open-shell systems.

quaterthienyl central part by ca. 0.030 *e* on going from the neutral form to the radical cation. These results indicate that the loss of electron density of the  $\pi$ -conjugated backbone is partially mitigated by the polarization of the C–H bonds. On the other hand, in the dicationic species the main differences are found for the hydrogens and the C <sub>$\beta$</sub>  atoms of the bithienyl end moieties and the vinylene spacers. As an example, the Mulliken atomic charges of the C<sub>1</sub>, C<sub>4</sub>, and C<sub>16</sub> atoms are larger (by 0.068, 0.058, and 0.091 *e*, respectively) than those of the neutral form, while the charges of the hydrogens show an overall increase by ca. 0.040 *e*. Also in the dication the C–H bonds are polarized due to the quinoidization of the molecule.

## VI. Conclusions

From the analysis of the Raman spectrum of a well-barrier-well vinylene-bridged-octithiophene in neutral state it is concluded that the effective  $\pi$ -conjugation significantly increases with respect to the corresponding vinylene-bridged-quaterthiophene monomer.

On the other hand, the spectroelectrochemical Raman study of the doped samples suggests that the full oxidation of this intercalated octathienyl cooligomer takes place in two steps: the generation, at low anodic potentials, of the radical cation, and, at high anodic potentials, of the dication. The theoretical HF/3-21G\* results indicate that the two ionized forms are characterized by the reversal of the single-double CC bonds alternation pattern with respect to the neutral molecule. The radical cation defect is mainly located over the quaterthienyl central part, while the dicationic defect strongly affects the whole structure of the molecule as a consequence of the electrostatic repulsion between the two positive-like charges.

**Acknowledgment.** The present work was supported in part by the Dirección General de Enseñanza Superior (DGES, MEC, Spain) through the research projects PB96-0682 and FD97-1765-C03. We are also indebted to Junta de Andalucía (Spain) for funding for our research group (FQM-0159). The authors acknowledge the use of the scientific instrumentation and the technical facilities of the Servicio de Apoyo a la Investigación (SCAI) of the University of Malaga.

## References and Notes

- (1) Kobayashi, T. *Nonlinear Optics of Organics and Semiconductors*; Springer: Berlin, 1989.
- (2) Chemla, D. S.; Zyss, J. *Nonlinear Optical Properties of Organics Molecules and Crystals*; Academic Press: New York, 1986; Vols. 1 and 2.
- (3) Garnier, F.; Hajlaoui, R.; Yassar, A.; Srivastava, P. *Science* **1994**, *265*, 1684.
- (4) Dodabalapur, A.; Katz, H. E.; Torsi, L.; Haddon, R. C. *Science* **1995**, *269*, 1560.
- (5) Spangler, C. V.; Liu, P. K. *Synth. Met.* **1991**, *44*, 259.
- (6) Fujii, A.; Kawahara, H.; Yoshida, M.; Ohmori, Y.; Yoshino, K. *J. Phys. D* **1995**, *28*, 2135.
- (7) Brouwer, H. J.; Krasnikov, V. V.; Hilberer, A.; Wildeman, J.; Hadzioannou, G. *Appl. Phys. Lett.* **1995**, *67*, 795.
- (8) Vanhatten, P. F.; Gill, R. E.; Herrema, J. K.; Hadzioannou, G. *J. Phys. Chem.* **1995**, *99*, 3932.
- (9) Müllen, K.; Wegner, G. *Electronic Materials: The Oligomer Approach*; Wiley-VCH: Weinheim, 1998.
- (10) Meyers, F.; Heeger, A. J.; Brédas, J. L. *J. Phys. Chem.* **1991**, *44*, 259.
- (11) Harada, I.; Furukawa, Y. *Vibrational Spectra and Structure*; Elsevier: Amsterdam, 1991.
- (12) Schaffer, H. E.; Chance, R. R.; Silbey, R. J.; Knoll, K.; Schrock, R. J. *Chem. Phys.* **1991**, *94*, 4161.
- (13) Castiglioni, C.; Gussoni, M.; López Navarrete, J. T.; Zerbi, G. *Solid State Commun.* **1988**, *65*, 625.
- (14) López Navarrete, J. T.; Zerbi, G. *J. Chem. Phys.* **1991**, *94*, 957 and 965.
- (15) Hernández, V.; Castiglioni, C.; del Zoppo, M.; Zerbi, G. *Phys. Rev. B* **1994**, *50*, 9815.
- (16) Ehrendorfer, Ch.; Karpfen, A. *J. Phys. Chem.* **1994**, *98*, 7492.
- (17) Onoda, M.; Morita, S.; Iwasa, T.; Nakayama, H.; Yoshino, K. *J. Chem. Phys.* **1991**, *95*, 8584.
- (18) Elendaloussi, E. H.; Frere, P.; Roncali, J. *J. Chem. Soc., Chem. Commun.* **1997**, 301.
- (19) Elendaloussi, E. H.; Frere, P.; Richomme, P.; Orduna, J.; Garín, J.; Roncali, J. *J. Am. Chem. Soc.* **1997**, *119*, 10774.
- (20) Hernández, V.; Casado, J.; Kanemitsu, Y.; López Navarrete, J. T. *J. Chem. Phys.* **1999**, *110*, 6907.
- (21) Casado, J.; Hernández, V.; Kanemitsu, Y.; López Navarrete, J. T. *J. Raman Spectrosc.* **2000**, *31*, 565.
- (22) Berlin, A.; Zotti, G. *Synth. Met.* **1999**, *106*, 197.
- (23) Casado, J.; Hernández, V.; Hotta, S.; López Navarrete, J. T. *J. Chem. Phys.* **1998**, *109*, 10419.
- (24) Pietro, W. J.; Francl, M. M.; Henhre, W. J.; Defrees, D. J.; Pople, J. A.; Binkley, J. S. *J. Am. Chem. Soc.* **1982**, *104*, 5039.
- (25) Frisch, M. J.; Trucks, G. W.; Schlegel, H. B.; Scuseria, G. E.; Robb, M. A.; Cheeseman, J. R.; Zakrzewski, V. G.; Montgomery, J. A.; Stratman, R. E.; Burant, S.; Dapprich, J. M.; Millam, J. M.; Daniels, A. D.; Kudin, K. N.; Strain, M. C.; Farkas, O.; Tomasi, J.; Barone, V.; Cossi, M.; Cammi, R.; Mennucci, B.; Pomelli, C.; Adamo, C.; Clifford, S.; Ochterski, G.; Petersson, A.; Ayala, P. Y.; Cui, Q.; Morokuma, K.; Malick, D. K.; Rabuck, A. D.; Raghavachari, K.; Foresman, J. B.; Cioslowski, J.; Ortiz, J. V.; Stefanov, B. B.; Liu, G.; Liashenko, A.; Piskorz, I.; Komaromi, I.; Gomperts, R.; Martin, R. L.; Fox, D. J.; Keith, T.; Al-Laham, M. A.; Peng, C. Y.; Manayakkara, A.; Gonzalez, C.; Challacombe, M.; Gill, P. M. W.; Johnson, B. G.; Chen, W.; Wong, M. W.; Andres, J. L.; Head-Gordon, M.; Replogle, E. S.; Pople, J. A. *Gaussian 98*, Revision A.7; Gaussian, Inc.: Pittsburgh, PA, 1998.
- (26) Louarn, G.; Mévéllec, J. Y.; Lefrant, S.; Buisson, J. P.; Fichou, D.; Teulade-Fichou, M. P. *Synth. Met.* **1995**, *69*, 351.
- (27) Agosti, E.; Rivola, M. L.; Hernández, V.; Zerbi, G. *Synth. Met.* **1999**, *100*, 101.
- (28) Hernández, V.; Casado, J.; Ramírez, F. J.; Zotti, G.; Hotta, S.; López Navarrete, J. T. *J. Chem. Phys.* **1996**, *104*, 9271.
- (29) Casado, J.; Hernández, V.; Ramírez, F. J.; Hotta, S.; López Navarrete, J. T. *Opt. Mater.* **1998**, *9*, 82.
- (30) Casado, J.; Hernández, V.; Hotta, S.; López Navarrete, J. T. *Adv. Mater.* **1998**, *10*, 1258.
- (31) *HandBook of Chemistry and Physics*; CRC Press: Florida, 1994.